ACS Chemical Neuroscience

Research Article

pubs.acs.org/chemneuro

Molecular Mechanism of HIV-1 Tat Interacting with Human Dopamine Transporter

Yaxia Yuan,[†,‡,⊥] Xiaoqin Huang,[‡,⊥] Narasimha M. Midde,[§] Pamela M. Quizon,[§] Wei-Lun Sun,[§] Jun Zhu,[§] and Chang-Guo Zhan*[,†,‡]

[†]Molecular Modeling and Biopharmaceutical Center and [‡]Department of Pharmaceutical Sciences, College of Pharmacy, University of Kentucky, 789 South Limestone Street, Lexington, Kentucky 40536, United States

[§]Department of Drug Discovery and Biomedical Sciences, South Carolina College of Pharmacy, University of South Carolina, Columbia, South Carolina 29208, United States

S *Supporting Information*

ABSTRACT: Nearly 70% of HIV-1-infected individuals suffer from HIV-associated neurocognitive disorders (HAND). HIV-1 transactivator of transcription (Tat) protein is known to synergize with abused drugs and exacerbate the progression of central nervous system (CNS) pathology. Cumulative evidence suggest that the HIV-1 Tat protein exerts the neurotoxicity through interaction with human dopamine transporter (hDAT) in the CNS. Through computational modeling and molecular dynamics (MD) simulations, we develop a three-dimensional (3D) structural model for HIV-1 Tat binding with hDAT. The model provides novel mechanistic insights concerning how HIV-1 Tat interacts with hDAT and inhibits dopamine uptake by hDAT. In particular, according to the computational modeling, Tat binds most favorably with the outward-open state of hDAT. Residues Y88, K92, and Y470 of hDAT are predicted to be key residues involved in the interaction between hDAT and Tat. The roles of these hDAT residues in the interaction with Tat are validated by experimental tests through site-directed mutagensis and dopamine uptake assays. The agreement between the computational and experimental data suggests that the computationally predicted hDAT−Tat binding mode and mechanistic insights are reasonable and provide a new starting point to design further pharmacological studies on the molecular mechanism of HIV-1-associated neurocognitive disorders.

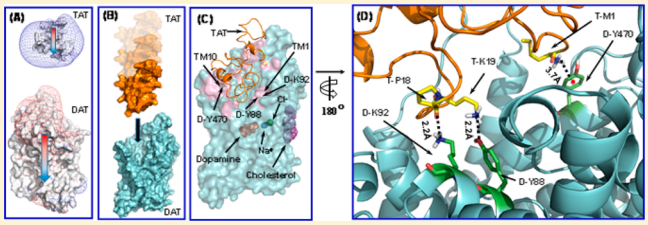

KEYWORDS: *Transactivator of transcription, protein−protein interaction, neurotoxicity, viral protein, dopamine uptake*

Human immunodeficiency virus (HIV) is a lentivirus causing the acquired immune deficiency syndrome (AIDS) disease.[1,2] According to the 2013 report of World Health Organization (WHO), a total number of 35.3 million people in the world are living with HIV/AIDS.[3] Among the genes of HIV virus, the transactivator of transcription (Tat) gene plays a role in the regulation of proteins that control how the HIV virus infects cells.[4−8] The HIV-1 positive cocaine abusers exhibit more serious neurological impairments, and they also have higher rates of motor and cognitive dysfunction compared with HIV-1 negative drug abusers.[9−12]

The Tat protein has been detected in the brain and the sera of HIV-1 patients.[13−15] Accumulating evidence[1,16−22] has revealed that HIV-1 Tat plays an important role in HIV-associated neurocognitive disorders (HAND) by disrupting intracellular communication.[23] Specifically, HIV-1 Tat exerts its neurotoxicity through interaction with some crucial proteins in the central nervous system (CNS), such as monoamine (dopamine, norepinephrine, and serotonin) transporters and *N*-methyl-D-aspartate (NMDA) receptors that are targets of some widely abused drugs including cocaine and methamphetamine. There have been extensive studies on these interactions and related problems.[9,19,20,22,24−42] We are particularly interested in human dopamine transporter (hDAT) due to our long-standing research interest in development of cocaine abuse-related medications[43−51] and the fact that hDAT is the primary target of cocaine in the CNS.[52,53] It has been reported that Tat and cocaine could synergistically impair hDAT function as demonstrated both in vivo[54] and in vitro.[1] Activity of presynaptic hDAT is strikingly reduced in HIV-1 patients with cocaine abuse.[30,55] As hDAT availability is correlated with HIV-1 associated neurocognitive deficits,[56,57] it has been estimated that ∼70% of HIV-1 patients are suffering from HAND.[6,7,18,21,58] The prevalence of HAND and the complicated connection of the HIV-1 infection with cocaine abuse have made a high priority in understanding molecular mechanism of HIV-1 Tat associated neurotoxicity. Understanding the detailed molecular mechanism concerning how the HIV-1 Tat interacts with hDAT could provide valuable clues to rationally design novel and effective therapeutics for treatment of HAND.

Received: January 2, 2015
Revised: January 26, 2015
Published: February 19, 2015

DOI: 10.1021/acschemneuro.5b00001
ACS Chem. Neurosci. 2015, 6, 658−665

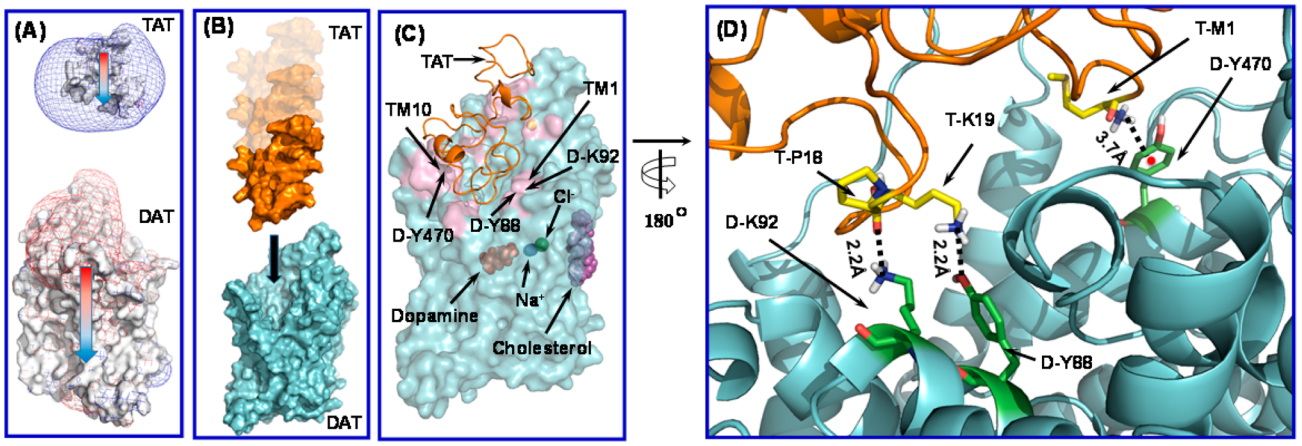

Figure 1. Simulated process of binding between HIV-1 Tat and hDAT in the outward-open state. (A) The HIV-1 Tat approaches hDAT through long-range electrostatic attractions, as indicated by the electrostatic potential contour maps for these two proteins. Isopotential surfaces are calculated at $+4k_BT/e$ for the positively charged surface (shown as blue mesh) and at $-3k_BT/e$ for the negatively charged surface (shown as red mesh), respectively. Colored arrows indicate the directions of the dipoles of both molecules. (B) The general process of two proteins approaching toward each other and form the initial encounter complex. Both proteins are represented as the surface style, with HIV-1 Tat in gold and hDAT in cyan. The black arrow indicates the HIV-1 Tat aligning to the vestibule near the extracellular side of hDAT. (C) Typical hDAT−Tat binding structure derived from the last snapshot of the MD trajectory #1 followed by the energy minimization. Tat is represented as gold ribbons. hDAT is represented by a semitransparent cyan surface. Substrate dopamine, cholesterol, sodium ions, chloride ion, and zinc ion are represented by the sphere style and colored in red, purple, blue, green, and yellow, respectively. The contact interface of hDAT between Tat and hDAT is colored in pink. It was observed that both TM10 and TM1 are involved in the interaction between Tat and hDAT. (D) Atomic interactions on the binding interface of the typical hDAT−Tat binding structure (as shown in C). HIV-1 Tat protein is shown as ribbon and colored in gold, and hDAT is shown as cyan ribbon. Residues T-M1, T-P18, and T-K19 of HIV-1 Tat are shown in ball−stick style and colored in yellow. Residues D-Y470, D-Y88, and D-K92 are shown in ball−stick style and colored in green. Dashed lines represent intermolecular hydrogen bonds with labeled distances. For D-Y470, the red point indicates the center of its aromatic ring, and the dashed line pointing to the red ball represents the cation-π interaction with labeled distance.

It has been known[20,22,59] that HAND-related abnormal neurocognitive function is associated with dysfunctions in dopamine (DA) neurotransmission. Protein hDAT picks up DA released from synaptic cleft and transports DA into presynaptic neurons.[60−62] The transporting process must be assisted by the binding of two Na^+ ions and one Cl^- ion, and it has been known that this process involves three typical conformational states of hDAT: outward-open state (i.e., the extracellular side of substrate-binding site for the transmitter is open, while the intracellular side is blocked); the outward-occluded state (i.e., both the extracellular and intracellular sides of binding site are blocked such that the binding site is occluded and no longer accessible for substrate); and the inward-open state (i.e., the intracellular side of substrate-binding site is open, while the extracellular side is blocked).[63−71]

The present study aims to understand how hDAT interacts with HIV-1 Tat at molecular level, particularly the detailed hDAT−Tat binding mode. It is a grand challenge to determine an X-ray crystal structure of hDAT−Tat binding complex in the physiological membrane environment. There is also no X-ray crystal structure available for hDAT itself. On the other hand, state-of-the-art molecular modeling techniques provide a useful tool to model the possible hDAT−Tat binding. Previous computational studies[64,72−75] provided homology models of hDAT concerning the general features of conformational changes during dopamine transporting process by hDAT. The obtained hDAT models allow to investigate how hDAT interacts with dopamine, cocaine, and other interesting ligands.[38,39] However, all of the previous studies, including those by our own group[38,40,76] were based on the hDAT models built through homology modeling using the previously available X-ray crystal structure of the bacterial homologue Leucine transporter ($LeuT_{Aa}$)[70] as a template, and the template $LeuT_{Aa}$ shares less than 25% sequence identity with hDAT. It is generally recognized that structural models derived from homology modeling will be reliable only when the template has a higher sequence identity and higher evolutionary homology with the modeled protein.

It is very interesting to note that an X-ray crystal structure has recently been determined for *drosophila* dopamine transporter (dDAT).[71] The sequences of dDAT and hDAT are very similar, with a sequence similarity reaching 59% (identity: 46%), which is considered rather high for homology modeling; in general, 40% sequence identity between a template protein and a target protein is considered sufficient for constructing a satisfactory homology model.[77,78] So, the newly available X-ray crystal structure of dDAT has become the most reasonable template for modeling the hDAT structures to be used in our studies on the hDAT structures and its binding with ligands. The newly built hDAT structures are consistent with all of the known structural insights obtained from previously reported wet-experimental validations on hDAT.[64,66,67,70,71] The more reasonable models of hDAT have allowed us to study how hDAT interacts with HIV-1 Tat. This is the first report on the use of the new hDAT models (based on the X-ray crystal structure of dDAT) to study the possible hDAT−Tat binding mode. The hDAT−Tat binding structure is determined through protein−protein docking[79] and molecular dynamics (MD) simulations.[80] Based on the determined hDAT−Tat binding structure, the HIV-1 Tat protein preferably binds with the outward-open state of hDAT, and critical residues contributing to the hDAT−Tat binding are identified. The computationally determined hDAT−Tat bind-

DOI: 10.1021/acschemneuro.5b00001
ACS Chem. Neurosci. 2015, 6, 658−665

ing mode has been validated by experimental tests including site-directed mutagenesis and DA uptake assays. The new insights obtained from the current study provide a structural basis for future extensive studies on the molecular mechanisms of HIV-1 Tat associated neurotoxicity and the relationship between HIV-1 infection and drug abuse.

RESULTS AND DISCUSSION

Binding Mode of HIV-1 Tat with hDAT. To determine the hDAT−Tat binding structure, we first need to know the detailed structures of both hDAT and HIV-1 Tat. The hDAT structures were built from the X-ray crystal structure of dDAT (PDB code: 4M48)[71] through homology modeling. The obtained structural model of hDAT are consistent with all of the known structural insights obtained from previously reported wet-experimental validations on hDAT.[64,66,67,70,71] In particular, the hDAT model has all of the previously known general features of hDAT including D476-R85 salt bridge, orientation of F320 residue, binding sites of dopamine, Zn^{2+}, Na^{+}, and Cl^{-}. Concerning HIV-1 Tat structure, B-type HIV-1 Tat (Tat Bru) is prevalent in North America and has 86 amino acids with a net charge of +12*e* at the physiological pH 7.4.[81] Multinuclear NMR spectroscopy revealed that the Tat Bru protein exists in a random coil conformation, and only transient folding can occur in its Cys-rich region (residues 22−37, see Figure S1 in Supporting Information) and its core region (residues 38−48). All of the 11 conformations of HIV-1 Tat obtained from NMR studies (PDB entry as 1JFW)[81] are quite similar, with the average positional root-mean square deviation (RMSD) of the backbone atoms being 1.3 Å. Starting from the NMR structures of HIV-1 Tat,[81] it is also important to know which one of the three conformational states of hDAT (i.e., the outward-open state, outward-occluded state, and inward-open state) are more favored for the binding with HIV-1 Tat protein. For this purpose, a protein−protein docking program, ZDOCK 3.0.2,[79] was used to explore possible hDAT−Tat complex structures (see Supporting Information for the computational details). As shown in Figure 1A, the calculated electrostatic potentials and the molecular dipole moments of both HIV-1 Tat and hDAT indicate that the long-range electrostatic attraction may act as a driving force for the association of these two proteins. Such obvious charge anisotropy between these two proteins drives HIV-1 Tat approaching to the mouth of the vestibule near the extracellular region of hDAT. This suggests that the HIV-1 Tat interacts directly with hDAT residues around the extracellular region of hDAT. Therefore, our protein−protein docking was focused on docking the HIV-1 Tat protein into the extracellular region for each of the three conformational states of hDAT, and a total of 3000 candidates (including all of the three possible conformational states of hDAT with various poses and conformations of HIV-1 Tat) were selected from all the docking results as initial complex structures. Further, as the rigid-body protein−protein docking cannot account for the conformational flexibility of the proteins, the initial complex structures obtained from the protein−protein docking were refined through a series of energy-minimizations, MD simulations, and molecular mechanics-Poisson−Boltzmann surface area (MM-PBSA)[82] binding energy calculations (see Supporting Information for the computational details) to capture the most favorable hDAT−Tat binding structure. Through the modeling and MD simulations, we were able to identify the best possible hDAT−Tat binding mode for each conformational state (outward-open, outward-occluded, or inward-open) of hDAT. According to the obtained binding structures and energies, HIV-1 Tat can bind with only the outward-open structure of hDAT due to the excellent geometrical match and favorable binding energy, and the outward-occluded and inward-open states cannot bind with HIV-1 Tat due to the bad geometrical match and unfavorable binding energies. Hence, our discussion below will focus on HIV-1 Tat binding with the outward-open state of hDAT.

For the most favorable hDAT−Tat binding mode (with hDAT in the outward-open state), we further carried out the final MD simulations for a total of 100 ns, including 10 independent MD trajectories with 10 ns for each. It turned out that the 10 trajectories (MD trajectories 1−10) led to very similar binding structures, which gives us further confidence in the MD-simulated hDAT−Tat binding mode. For convenience, the specific hDAT−Tat binding structure discussed below will always refer to the MD trajectory no. 1, unless explicitly stated otherwise. Figure 1B depicts the general process of the hDAT−Tat binding, that is, the HIV-1 Tat molecule diffuses around the extracellular side of hDAT (colored in cyan), and forms an initial encounter complex with hDAT due to the electrostatic attraction, according to the computational modeling. Conformational adjustments around the binding interface lead to the formation of the final hDAT−Tat binding structure. Figure 1C represents a typical complex structure of HIV-1 Tat binding with the outward-open state of hDAT, which is derived from the last snapshot of the 10 ns MD trajectory. The HIV-1 Tat molecule sits just above the vestibule near the extracellular side of hDAT, and it forms a contacting interface which involves residues D-Y88, D-K92, and D-Y470. Such orientation of HIV-1 Tat will certainly block the entry pathway of substrate DA and, therefore, inhibit the transporting of DA by hDAT. Figure 1D depicts the critical intermolecular interactions as observed from this hDAT−Tat binding structure (Figure 1C). Specifically, these critical interactions include: the cation-π interaction between the positively charged amino-group of T-M1 at the N-terminus of HIV-1 Tat and the aromatic D-Y470 side chain of hDAT; the hydrogen bonding interaction between the positively charged headgroup of T-K19 side chain and the hydroxyl group of D-Y88 side chain; and the hydrogen bonding interaction between the backbone oxygen atom of T-P18 and the positively charged headgroup of D-K92 side chain. Depicted in Figure 2 are the tracked time-dependent distances of these critical intermolecular interactions and the positional RMSD for all backbone atoms of the MD-simulated hDAT−Tat complex in 10 MD trajectories for a total of 100 ns. As shown in Figure 2, the RMSD values for all of the 10 MD trajectories are around 2.11 ± 0.24 Å with small fluctuations, suggesting a high conformational stability of the hDAT−Tat binding structure. As shown in Figure 2, the cation-π interaction between T-M1 and D-Y470 had an average distance of 4.13 ± 0.35 Å (green curve), a weak hydrogen bond between T-K19 and D-Y88 had an average H···O distance of 2.52 ± 0.31 Å (blue curve), and another weak hydrogen bond between T-P18 and D-K92 had an average O···H distance of 2.33 ± 0.46 Å (red curve). These tracked distances suggest that all these hDAT−Tat interactions are persistent throughout the MD simulations.

Validation of the Predicted hDAT−Tat Binding Mode. For validation of the computationally predicted hDAT−Tat binding structure, we also carried out wet experimental studies including site-directed mutagenesis and DA-uptake assay (see

DOI: 10.1021/acschemneuro.5b00001
ACS Chem. Neurosci. 2015, 6, 658−665

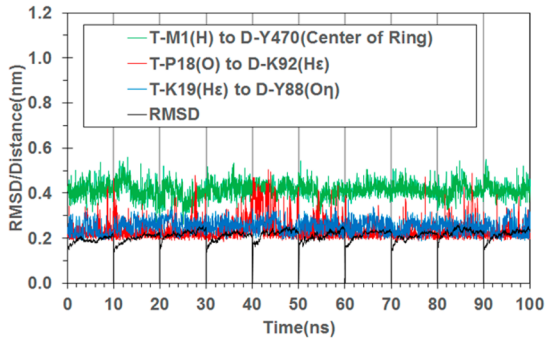

Figure 2. Tracked changes of critical distances and positional RMSD values for the hDAT−Tat binding structure based on the 10 MD trajectories (10 ns for each MD trajectory). Green curve refers to the distance between the positively charged amino group of T-M1 of HIV-1 Tat and the center of the aromatic ring at D-Y470 side chain. Blue curve represents the distance between the hydrogen atom on the positively charged head of T-K19 side chain and the hydroxyl oxygen atom of D-Y88 side chain, and the red curve refers to the distance between the backbone oxygen atom of T-P18 and the hydrogen atom on the positively charged head of D-K92 side chain. The black curve refers to the positional RMSD for the backbone atoms of the hDAT−Tat binding complex.

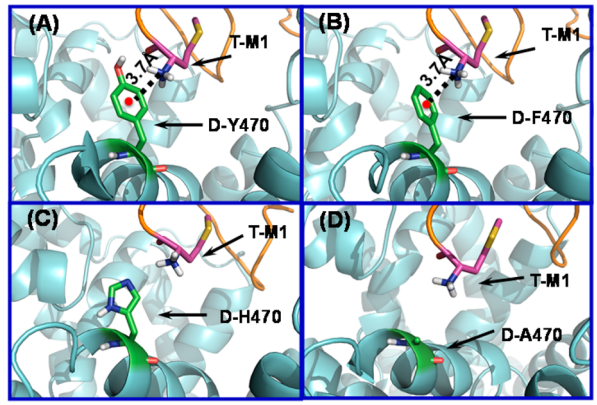

Figure 3. Interactions between the positively charged amino group of T-M1 and the side chain of residue no. 470 of hDAT in the modeled complexes of HIV-1 Tat binding with WT-hDAT and its mutants. Structures of the Y470F, Y470H, and Y470A mutants of hDAT were modeled starting from that of WT-hDAT in the hDAT−Tat binding structure shown in Figure 1C and 1D by changing the Y470 side chain into the corresponding one of the mutant and then performing the energy minimization. (A) Residues T-M1 and D-Y470 are represented as sticks and colored by atom types. The red point represents the center of aromatic ring of residue no. 470 of hDAT, and the dashed line pointing to the red point represents the cation-π interaction with the distance labeled. (B) Y470F mutation retains the cation-π interaction between T-M1 and D-F470. The distance between the center of aromatic side chain of D-F470 and the nitrogen atom of the positively charged amino group of T-M1 is indicated in Å. (C) Residue D-H470 stays far away from the positively charged amino group of T-M1 (i.e., no direct cation-π interaction). (D) Residue D-A470 stays further away from the positively charged amino group of T-M1 (i.e., no direct cation-π interaction).

the Methods section below; more extensive experimental assays and data will be reported elsewhere) to determine the inhibitory effects of Tat on several hDAT mutants (including the Y470F, Y470H, Y470A, Y88F, and K92M mutants) in comparison with wild-type hDAT (WT-hDAT).

According to the hDAT−Tat binding structure (Figures 1 and 2), there is a strong cation-π interaction between the positively charged amino group of T-M1 (i.e., M1 of HIV-1 Tat) and the aromatic ring of D-Y470 (i.e., Y470 of hDAT) side chain. Therefore, mutation of D-Y470 to phenylalanine should not weaken the favorable cation-π interaction, but mutation of D-Y470 to any other amino acid without the aromatic ring would significantly decrease the hDAT−Tat binding and the inhibitory effect of Tat on hDAT, as seen in Figure 3.

All of these computational insights are supported by the experimental data depicted in Figure 4. Experimental data (Figure 4A) revealed that, compared to their respective controls, exposure to Tat_{1-86} significantly decreased [^{3}H]DA uptake in WT-hDAT by 33.0% and Y470F-hDAT by 37.6%, respectively; however, nearly negligible effects of Tat were observed in Y470H-hDAT, Y470A-hDAT, Y88F-hDAT, and K92M-hDAT. In addition, the Tat-mediated inhibitory effects on DA uptake were also expressed as a percent change from the DA uptake in WT-hDAT (100%) in the presence of Tat. As illustrated in Figure 4B, the Tat-induced inhibitory effect on DA uptake was dramatically reduced in Y470H-hDAT, Y470A-hDAT, Y88F-hDAT, and K92M-hDAT, suggesting that these mutants significantly attenuate Tat-induced inhibition of DA uptake.

As seen in Figure 4B, the Y470H and Y470A mutations on hDAT did decrease the inhibitory effect of Tat by ∼85% and ∼49%, respectively, and the Y470F mutation did not decrease the inhibitory effect of Tat at all. These experimental activity data strongly support the computationally predicted important role of the aromatic ring of D-Y470 side chain (see Figure 3A). The Y470F mutant of hDAT still has the aromatic side chain (see Figure 3B), which explains why the Y470F mutation did not decrease the inhibitory effect of Tat at all. In fact, the Y470F mutation slightly increased the inhibitory effect (by ∼14%). The Y470F mutation-induced slight increase in the inhibitory effect of Tat suggests that the cation-π interaction between the positively charged amino group of T-M1 and the aromatic ring (of D-Y470 side chain) becomes slightly stronger after the hydroxyl group on the aromatic ring is removed.

The Y470A mutation on hDAT changes the aromatic side chain of D-Y470 to a much smaller one (methyl group) and, thus, removes the favorable cation-π interaction (see Figure 3D), which explains why the Y470A mutation significantly decreased the inhibitory effect of Tat (by ∼49%). The Y470H mutation not only removes the favorable cation-π interaction but also produces unfavorable contacts with the positively charged amino group of T-M1, and thus, the H470 side chain was pushed away from the positively charged amino group of T-M1 during the modeling process (see Figure 3C), which explains why the Y470H mutation even more significantly decreased the inhibitory effect of Tat (by ∼85%) compared to the Y470A mutation (∼49%).

In addition, Y88 and K92 of hDAT (i.e., D-Y88 and D-K92) are also predicted to be critical residues interacting with Tat through forming hydrogen bonds with K19 and P18 of Tat (i.e., T-K19 and T-P18), respectively (see Figures 1D and 2). So, the Y88F or K92M mutation on hDAT would decrease the hDAT−Tat binding and the inhibitory effect of Tat on hDAT. The experimental data in Figure 4B show that the Y88F and K92M mutations on hDAT indeed significantly decreased the inhibitory effect of Tat by ∼67% and ∼54%, respectively, supporting the favorable roles of the D-Y88 and D-K92 side chains. The agreement between the computational and

DOI: 10.1021/acschemneuro.5b00001
ACS Chem. Neurosci. 2015, 6, 658−665

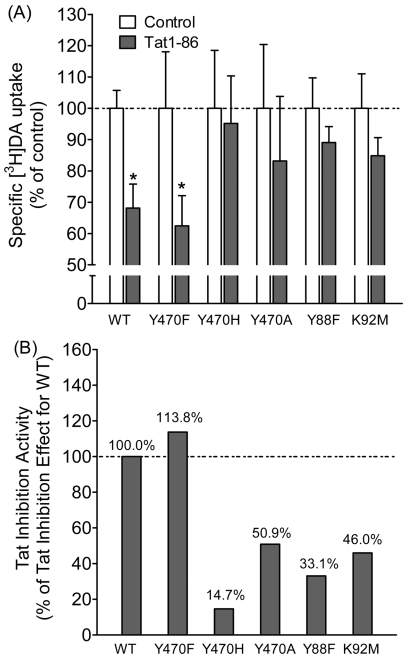

Figure 4. Effects of Tat on the kinetic analysis of [^{3}H]DA uptake by WT-hDAT and its mutants. (A) PC12 cells transfected with WT-hDAT (WT) Y470F-hDAT (Y470F), Y470H-hDAT (Y470H), Y470A-hDAT (Y470A), Y88F-hDAT (Y88F), or K92M-hDAT (K92M) were preincubated with or without recombinant Tat_{1-86} (500 nM, final concentration) at room temperature for 20 min followed by the addition of 0.05 μM final concentration of the [^{3}H]DA. *$p < 0.05$ compared to respective control in the absence of Tat ($n = 4$). (B) The corresponding Tat-induced inhibitory effects on [^{3}H]DA uptake in hDAT mutants were presented as the percentage of the Tat-induced inhibitory effect of [^{3}H]DA uptake in WT-hDAT (100%) at the same concentrations of [^{3}H]DA (0.05 μM) and Tat_{1-86} (500 nM).

experimental data suggests that the computationally determined hDAT−Tat binding mode is reasonable.

Lastly, we would like to point out that understanding the molecular mechanism for hDAT−Tat interaction is the first step of the more extensive efforts that aim to understand how Tat interacts with other transporters and receptors in the CNS. The similar integrated computational strategy used in this report may be used to explore the structural models concerning how Tat interacts with other transporters and receptors. Understanding the detailed molecular mechanisms for Tat interacting with all of the relevant transporters and receptors, one could eventually have a chance to explore possible therapeutic agents that can block Tat binding with multiple transporters/receptors to combat HAND.

CONCLUSION

We have developed a reasonable 3D structural model of hDAT binding with HIV-1 Tat through protein−protein docking and molecular dynamics simulations. According to the computational data, HIV-1 Tat binds most favorably with the outward-open state of hDAT. Based on the modeled hDAT−Tat binding struture, residues Y88, K92, and Y470 of hDAT are predicted to be key residues for hDAT interacting with Tat. The computational predictions are supported by experimental tests including site-directed mutagenesis and dopamine uptake assays in the presence and absence of Tat. The good agreement between the computational and experimental data suggests that the computationally predicted hDAT−Tat binding mode is reasonable. The newly obtained hDAT−Tat binding mode provides novel mechanistic insights concerning how HIV-1 Tat interacts with hDAT and inhibits the dopamine transporting in hDAT. Starting from the new hDAT−Tat binding mode and mechanistic insights, one may design further studies to explore the more detailed molecular mechanisms and develop potentially effective therapeutics for treatment of HIV-1 associated neurocognitive disorders. In general, this study also demonstrates how the complex structural and mechanistic questions concerning protein−protein interactions can be addressed by using a generally applicable strategy including integrated computational-experimental studies.

METHODS

Molecular Modeling. In order to dock HIV-1 Tat protein into the possible binding site on the extracellular side of hDAT, and to build the initial hDAT−Tat binding structure, protein−protein docking was performed by using the ZDOCK 3.0.2 program.[79] The 11 conformations of HIV-1 Tat based on NMR structural analysis[81] were all treated equally as the ligand protein, and structures of the three conformational states of hDAT (generated by the Modeler module of Discovery 2.5[83] and energy-optimized using the AMBER 12 software package[80]) were treated as the receptor protein. For each of the three conformational states of hDAT (i.e., the outward-open, outward-occluded, and inward-open states), 10 snapshots were selected with a 1 ns interval from a 10 ns trajectory of molecular dynamics (MD) simulations in the production stage. In order to probe whether there is a charge anisotropy between these two proteins, the electrostatic potentials and the molecular dipole moments for both HIV-1 Tat and hDAT were calculated by using the PDB2PQR server.[84] Because the HIV-1 Tat bears positive electrostatic potential on its surface, and the hDAT bears negative electrostatic potential on the surface of its extracellular side, these two proteins are expected to electrostatically attract each other along the direction of their dipole moments. Based on this piece of information, it is reasonable to assume that the HIV-1 Tat would probably bind with hDAT at a site around the extracellular region of hDAT. During the protein−protein docking process, the rotational sampling (with 6° angular sampling) method implemented in the ZDOCK 3.0.2 was used in order to make a more complete configuration sampling for these two proteins. The score function of ZRANK[85] program was used to score the binding energy between the ligand protein (HIV-1 Tat) and the receptor protein (hDAT). For each protein−protein docking, the program was set to output top-2000 candidates as the possible binding complexes. The docking of 11 HIV-1 Tat conformations into the hDAT structures associated with the 10 MD snapshots (i.e., 10 conformations) for each conformational state of hDAT (e.g., the outward-open state) generated 11 × 10 × 2000 = 220 000 candidates of the binding structure. Considering that the HIV-1 Tat should contact directly with residues around the mouth of the vestibule near the extracellular end of hDAT structure (as this vestibule and the substrate-entry pathway were explored in our previous studies on the homology modeling of hDAT and its inhibition by (−)-cocaine[72,74]), we ruled out all candidate complexes that do not directly align with the residues around the mouth of the vestibule of hDAT. This initial screening reduced the 220 000 candidates to 1000 candidates of HIV-1 binding with the outward-open state of hDAT. Such protein−protein docking and initial screening were also performed for the 11 HIV-1 Tat conformations docking with the 10 MD snapshots of the outward-occluded state of hDAT, and then docking with the 10 MD snapshots of the inward-open state of hDAT. The total number of the selected candidates for HIV-1 Tat binding with all three conformational states of hDAT became 3000 (i.e., 1000 + 1000 + 1000). These 3000 candidates were subjected to further MD simulations and binding energy calculations (see Supplemental Data for the computational details), and lastly, the most favorable binding structure was determined with the lowest binding energy.

DOI: 10.1021/acschemneuro.5b00001
ACS Chem. Neurosci. 2015, 6, 658−665

Construction of Plasmids. All point mutations of Tyr88, Lys92, and Tyr470 in hDAT were selected on the basis of the predictions of the 3D-computational modeling and simulations. All mutations in hDAT were generated based on wild-type human DAT (WT-hDAT) sequence (NCBI, cDNA clone MGC: 164608 IMAGE: 40146999) by site-directed mutagenesis. Synthetic cDNA encoding hDAT subcloned into pcDNA3.1+ (provided by Dr. Haley E Melikian, University of Massachusetts) was used as a template to generate mutants using QuikChange site-directed mutagenesis Kit (Agilent Tech, Santa Clara CA). The sequence of the mutant construct was confirmed by DNA sequencing at University of South Carolina EnGenCore facility. Plasmids DNA were propagated and purified using plasmid isolation kit (Qiagen, Valencia, CA, U.S.A.).

Cell Culture and DNA Transfection. Pheochromocytoma (PC12, ATCC no. CRL-1721) cells were maintained in Dulbecco's modified eagle medium supplemented with 15% horse serum, 2.5% bovine calf serum, 2 mM glutamine and antibiotics (100 U/ml penicillin and 100 μg/mL streptomycin). Both cells were cultured at 37 °C in a 5% CO_2 incubator. For hDAT (wild-type or mutant) transfection, cells were seeded into 24 well plates at a density of 1×10^5 cells/well. After 24 h, cells were transfected with WT or mutant hDAT plasmids using Lipofectamine 2000 (Life Tech, Carlsbad, CA). Cells were used for the experiments after 24 h of transfection.

[^{3}H]DA Uptake Assay. Twenty-four hours after transfection, [^{3}H]DA uptake in PC12 cells transfected with WT-hDAT and mutants was performed, as reported previously.[76] To determine whether Tat inhibits DA uptake, kinetic analyses of [^{3}H]DA uptake were conducted in WT-hDAT and its mutants in the absence or presence of Tat. In brief, [^{3}H]DA uptake was measured in Krebs-Ringer-HEPES (KRH) buffer (final concentration in mM: 125 NaCl, 5 KCl, 1.5 $MgSO_4$, 1.25 $CaCl_2$, 1.5 KH_2PO_4, 10 D-glucose, 25 HEPES, 0.1 EDTA, 0.1 pargyline, and 0.1 L-ascorbic acid; pH 7.4) containing one of six concentrations of unlabeled DA (final DA concentrations, 1.0 nM−5 μM) and a fixed concentration of [^{3}H]DA (500,000 dpm/well, specific activity, 21.2 Ci/mmol; PerkinElmer Life and Analytical Sciences, Boston, MA). In parallel, nonspecific uptake of each concentration of [^{3}H]DA (in the presence of 10 μM nomifensine, final concentration) was subtracted from total uptake to calculate DAT-mediated uptake. To determine the inhibitory effects of Tat on [^{3}H]DA uptake, cells transfected with WT hDAT or mutant were preincubated with or without Tat_{1-86} (500 nM, final concentration) at room temperature for 20 min followed by addition of [^{3}H]DA for an additional 8 min. The reaction was conducted at room temperature for 8 min and terminated by washing twice with ice cold uptake buffer. Cells were lysed in 500 μL of 1% SDS for an hour and radioactivity was measured using a liquid scintillation counter (model Tri-Carb 2900TR; PerkinElmer Life and Analytical Sciences, Waltham, MA). Kinetic data were analyzed using Prism 5.0 (GraphPad Software Inc., San Diego, CA).

■ ASSOCIATED CONTENT

Supporting Information

Figure S1 for amino acid sequence of B-type HIV-1 Tat (Tat Bru) protein. This material is available free of charge via the Internet at http://pubs.acs.org.

■ AUTHOR INFORMATION

Corresponding Author

*E-mail: zhan@uky.edu. Tel: 859-323-3943.

Author Contributions

⊥Y.Y. and X.H. contributed equally to this work.

Notes

The authors declare no competing financial interest.

■ ACKNOWLEDGMENTS

This work was supported in part by the NIH (grants R01 DA035714, R01 DA035552, R01 DA032910, and R01 DA025100) and the NSF (grant CHE-1111761). The authors acknowledge the Computer Center at the University of Kentucky for supercomputing time on a Dell Supercomputer Cluster consisting of 388 nodes or 4816 processors.

■ REFERENCES

(1) Ferris, M. J., Frederick-Duus, D., Fadel, J., Mactutus, C. F., and Booze, R. M. (2009) The human immunodeficiency virus-1−associated protein, Tat1−86, impairs dopamine transporters and interacts with cocaine to reduce nerve terminal function: A no-net-flux microdialysis study. *Neuroscience 159*, 1292−1299.

(2) Valdiserri, R. O. (2011) Commentary: Thirty Years of AIDS in America: A Story of Infinite Hope. *AIDS Educ. Prev. 23*, 479−494.

(3) Joint United Nations Programme on HIV/AIDS (UNAIDS) (2013) *Global report: UNAIDS report on the global AIDS epidemic 2013*, UNAIDS, Geneva.

(4) Silvers, J. M., Aksenov, M. Y., Aksenova, M. V., Beckley, J., Olton, P., Mactutus, C. F., and Booze, R. M. (2006) Dopaminergic marker proteins in the substantia nigra of human immunodeficiency virus type 1-infected brains. *J. Neurovirol. 12*, 140−145.

(5) Wallace, D. R., Dodson, S., Nath, A., and Booze, R. M. (2006) Estrogen attenuates gp120-and tat1−72-induced oxidative stress and prevents loss of dopamine transporter function. *Synapse 59*, 51−60.

(6) Li, W., Li, G., Steiner, J., and Nath, A. (2009) Role of Tat protein in HIV neuropathogenesis. *Neurotox. Res. 16*, 205−220.

(7) Ernst, T., Yakupov, R., Nakama, H., Crocket, G., Cole, M., Watters, M., Ricardo-Dukelow, M. L., and Chang, L. (2009) Declined neural efficiency in cognitively stable human immunodeficiency virus patients. *Ann. Neurol. 65*, 316−325.

(8) Carey, A. N., Sypek, E. I., Singh, H. D., Kaufman, M. J., and McLaughlin, J. P. (2012) Expression of HIV-Tat protein is associated with learning and memory deficits in the mouse. *Behav. Brain Res. 229*, 48−56.

(9) Ferris, M. J., Mactutus, C. F., and Booze, R. M. (2008) Neurotoxic profiles of HIV, psychostimulant drugs of abuse, and their concerted effect on the brain: current status of dopamine system vulnerability in NeuroAIDS. *Neurosci. Biobehav. Rev. 32*, 883−909.

(10) Nath, A. (2010) Human immunodeficiency virus-associated neurocognitive disorder: pathophysiology in relation to drug addiction. *Ann. N.Y. Acad. Sci. 1187*, 122−128.

(11) Zhu, J., Ananthan, S., Mactutus, C. F., and Booze, R. M. (2011) Recombinant human immunodeficiency virus-1 transactivator of transcription1−86 allosterically modulates dopamine transporter activity. *Synapse 65*, 1251−1254.

(12) Paris, J. J., Carey, A. N., Shay, C. F., Gomes, S. M., He, J. J., and McLaughlin, J. P. (2013) Effects of conditional central expression of HIV-1 Tat protein to potentiate cocaine-mediated psychostimulation and reward among male mice. *Neuropsychopharmacology 39*, 380−388.

(13) Del Valle, L., Croul, S., Morgello, S., Amini, S., Rappaport, J., and Khalili, K. (2000) Detection of HIV-1 Tat and JCV capsid protein, VP1, in AIDS brain with progressive multifocal leukoencephalopathy. *J. Neurovirol. 6*, 221−228.

(14) Hudson, L., Liu, J., Nath, A., Jones, M., Raghavan, R., Narayan, O., Male, D., and Everall, I. (2000) Detection of the human immunodeficiency virus regulatory protein tat in CNS tissues. *J. Neurovirol. 6*, 145−155.

(15) Lamers, S. L., Salemi, M., Galligan, D. C., Morris, A., Gray, R., Fogel, G., Zhao, L., and McGrath, M. S. (2010) Human immunodeficiency virus-1 evolutionary patterns associated with pathogenic processes in the brain. *J. Neurovirol. 16*, 230−241.

(16) Aksenova, M. V., Silvers, J. M., Aksenov, M. Y., Nath, A., Ray, P. D., Mactutus, C. F., and Booze, R. M. (2006) HIV-1 Tat neurotoxicity in primary cultures of rat midbrain fetal neurons: changes in dopamine transporter binding and immunoreactivity. *Neurosci. Lett. 395*, 235−239.

(17) Zhu, J., and Reith, M. E. A. (2008) Role of dopamine transporter in the action of psychostimulants, nicotine, and other drugs of abuse. *CNS Neurol. Disord. Drug Targets 7*, 393−409.

DOI: 10.1021/acschemneuro.5b00001
ACS Chem. Neurosci. 2015, 6, 658−665

(18) Zhu, J., Mactutus, C. F., Wallace, D. R., and Booze, R. M. (2009) HIV-1 Tat protein-induced rapid and reversible decrease in [3H]-dopamine uptake: dissociation of [3H]dopamine uptake and [3H]-2beta-carbomethoxy-3-beta-(4-fluorophenyl)tropane (WIN 35,428) binding in rat striatal synaptosomes. *J. Pharmacol. Exp. Ther. 329*, 1071−1083.
(19) Ferris, M. J., Frederick-Duus, D., Fadel, J., Mactutus, C. F., and Booze, R. M. (2010) Hyperdopaminergic tone in HIV-1 protein treated rats and cocaine sensitization. *J. Neurochem. 115*, 885−896.
(20) Purohit, V., Rapaka, R., and Shurtleff, D. (2011) Drugs of abuse, dopamine, and HIV-associated neurocognitive disorders/HIV-associated dementia. *Mol. Neurobiol. 44*, 102−110.
(21) Midde, N. M., Gomez, A. M., and Zhu, J. (2012) HIV-1 Tat protein decreases dopamine transporter cell surface expression and vesicular monoamine transporter-2 function in Rat striatal synaptosomes. *J. Neuroimmune Pharmacol. 7*, 629−639.
(22) Bagashev, A., and Sawaya, B. E. (2013) Roles and functions of HIV-1 Tat protein in the CNS: an overview. *Virol. J. 10*, 358.
(23) Kim, J., Yoon, J.-H., and Kim, Y.-S. (2013) HIV-1 Tat interacts with and regulates the localization and processing of amyloid precursor protein. *PLoS One 8*, e77972.
(24) Heaton, R. K., Clifford, D. B., Franklin, D. R., Jr., Woods, S. P., Ake, C., Vaida, F., Ellis, R. J., Letendre, S. L., Marcotte, T. D., Atkinson, J. H., Rivera-Mindt, M., Vigil, O. R., Taylor, M. J., Collier, A. C., Marra, C. M., Gelman, B. B., McArthur, J. C., Morgello, S., Simpson, D. M., McCutchan, J. A., Abramson, I., Gamst, A., Fennema-Notestine, C., Jernigan, T. L., Wong, J., Grant, I., and Group, C. (2010) HIV-associated neurocognitive disorders persist in the era of potent antiretroviral therapy: CHARTER Study. *Neurology 75*, 2087−2096.
(25) Gaskill, P. J., Calderon, T. M., Luers, A. J., Eugenin, E. A., Javitch, J. A., and Berman, J. W. (2009) Human immunodeficiency virus (HIV) infection of human macrophages is increased by dopamine: a bridge between HIV-associated neurologic disorders and drug abuse. *Am. J. Pathol. 175*, 1148−1159.
(26) Buckner, C. M., Luers, A. J., Calderon, T. M., Eugenin, E. A., and Berman, J. W. (2006) Neuroimmunity and the blood-brain barrier: molecular regulation of leukocyte transmigration and viral entry into the nervous system with a focus on neuroAIDS. *J. Neuroimmune Pharmacol. 1*, 160−181.
(27) Nath, A., Maragos, W. F., Avison, M. J., Schmitt, F. A., and Berger, J. R. (2001) Acceleration of HIV dementia with methamphetamine and cocaine. *J. Neurovirol. 7*, 66−71.
(28) Meade, C. S., Conn, N. A., Skalski, L. M., and Safren, S. A. (2011) Neurocognitive impairment and medication adherence in HIV patients with and without cocaine dependence. *J. Behav. Med. 34*, 128−138.
(29) Meade, C. S., Lowen, S. B., MacLean, R. R., Key, M. D., and Lukas, S. E. (2011) fMRI brain activation during a delay discounting task in HIV-positive adults with and without cocaine dependence. *Psychiatry Res. 192*, 167−175.
(30) Chang, L., Wang, G.-J., Volkow, N. D., Ernst, T., Telang, F., Logan, J., and Fowler, J. S. (2008) Decreased brain dopamine transporters are related to cognitive deficits in HIV patients with or without cocaine abuse. *Neuroimage 42*, 869−878.
(31) Kumar, A. M., Ownby, R. L., Waldrop-Valverde, D., Fernandez, B., and Kumar, M. (2011) Human immunodeficiency virus infection in the CNS and decreased dopamine availability: relationship with neuropsychological performance. *J. Neurovirol. 17*, 26−40.
(32) Berger, J. R., and Arendt, G. (2000) HIV dementia: the role of the basal ganglia and dopaminergic systems. *J. Psychopharmacol. 14*, 214−221.
(33) Sardar, A. M., Czudek, C., and Reynolds, G. P. (1996) Dopamine deficits in the brain: the neurochemical basis of parkinsonian symptoms in AIDS. *Neuroreport 7*, 910−912.
(34) Kumar, A. M., Fernandez, J. B., Singer, E. J., Commins, D., Waldrop-Valverde, D., Ownby, R. L., and Kumar, M. (2009) Human immunodeficiency virus type 1 in the central nervous system leads to decreased dopamine in different regions of postmortem human brains. *J. Neurovirol. 15*, 257−274.
(35) Scheller, C., Arendt, G., Nolting, T., Antke, C., Sopper, S., Maschke, M., Obermann, M., Angerer, A., Husstedt, I. W., Meisner, F., Neuen-Jacob, E., Muller, H. W., Carey, P., Ter Meulen, V., Riederer, P., and Koutsilieri, E. (2010) Increased dopaminergic neurotransmission in therapy-naive asymptomatic HIV patients is not associated with adaptive changes at the dopaminergic synapses. *J. Neural. Transm. 117*, 699−705.
(36) Beuming, T., Kniazeff, J., Bergmann, M. L., Shi, L., Gracia, L., Raniszewska, K., Newman, A. H., Javitch, J. A., Weinstein, H., Gether, U., and Loland, C. J. (2008) The binding sites for cocaine and dopamine in the dopamine transporter overlap. *Nat. Neurosci. 11*, 780−789.
(37) Koutsilieri, E., Czub, S., Scheller, C., Sopper, S., Tatschner, T., Stahl-Hennig, C., ter Meulen, V., and Riederer, P. (2000) Brain choline acetyltransferase reduction in SIV infection. An index of early dementia? *Neuroreport 11*, 2391−2393.
(38) Koutsilieri, E., ter Meulen, V., and Riederer, P. (2001) Neurotransmission in HIV associated dementia: a short review. *J. Neural. Transm. 108*, 767−775.
(39) Ernst, T., Jiang, C. S., Nakama, H., Buchthal, S., and Chang, L. (2010) Lower brain glutamate is associated with cognitive deficits in HIV patients: a new mechanism for HIV-associated neurocognitive disorder. *J. Magn. Reson. Imaging 32*, 1045−1053.
(40) Ferrarese, C., Aliprandi, A., Tremolizzo, L., Stanzani, L., De Micheli, A., Dolara, A., and Frattola, L. (2001) Increased glutamate in CSF and plasma of patients with HIV dementia. *Neurology 57*, 671−675.
(41) Aksenov, M. Y., Aksenova, M., Mactutus, C., and Booze, R. M. (2012) D1/NMDA receptors and concurrent methamphetamine+HIV-1 Tat neurotoxicity. *J. Neuroimmune Pharmacol. 7*, 599−608.
(42) S Silverstein, P., Shah, A., Weemhoff, J., Kumar, S., P Singh, D., and Kumar, A. (2012) HIV-1 gp120 and drugs of abuse: interactions in the central nervous system. *Curr. HIV Res. 10*, 369−383.
(43) Hamza, A., Cho, H., Tai, H.-H., and Zhan, C.-G. (2005) Molecular Dynamics Simulation of Cocaine Binding with Human Butyrylcholinesterase and Its Mutants. *J. Phys. Chem. B 109*, 4776−4782.
(44) Pan, Y., Gao, D., Yang, W., Cho, H., Yang, G., Tai, H.-H., and Zhan, C.-G. (2005) Computational redesign of human butyrylcholinesterase for anticocaine medication. *Proc. Natl. Acad. Sci. U.S.A. 102*, 16656−16661.
(45) Gao, D., Cho, H., Yang, W., Pan, Y., Yang, G., Tai, H.-H., and Zhan, C.-G. (2006) Computational Design of a Human Butyrylcholinesterase Mutant for Accelerating Cocaine Hydrolysis Based on the Transition-State Simulation13. *Angew. Chem. 118*, 669−673.
(46) Pan, Y., Gao, D., Yang, W., Cho, H., and Zhan, C.-G. (2007) Free Energy Perturbation (FEP) Simulation on the Transition States of Cocaine Hydrolysis Catalyzed by Human Butyrylcholinesterase and Its Mutants. *J. Am. Chem. Soc. 129*, 13537−13543.
(47) Zheng, F., Yang, W., Ko, M.-C., Liu, J., Cho, H., Gao, D., Tong, M., Tai, H.-H., Woods, J. H., and Zhan, C.-G. (2008) Most Efficient Cocaine Hydrolase Designed by Virtual Screening of Transition States. *J. Am. Chem. Soc. 130*, 12148−12155.
(48) Zhan, C.-G., Zheng, F., and Landry, D. W. (2003) Fundamental reaction mechanism for cocaine hydrolysis in human butyrylcholinesterase. *J. Am. Chem. Soc. 125*, 2462−2474.
(49) Zheng, F., Xue, L., Hou, S., Liu, J., Zhan, M., Yang, W., and Zhan, C.-G. (2014) A highly efficient cocaine detoxifying enzyme obtained by computational design. *Nat. Commun. 5*, Article no. 3457.
(50) Gao, D., Narasimhan, D. L., Macdonald, J., Ko, M.-C., Landry, D. W., Woods, J. H., Sunahara, R. K., and Zhan, C.-G. (2009) Thermostable variants of cocaine esterase for long-time protection against cocaine toxicity. *Mol. Pharmacol. 75*, 318−323.
(51) Fang, L., Chow, K. M., Hou, S., Xue, L., Rodgers, D. W., Zheng, F., and Zhan, C.-G. (2014) Rational design, preparation, and characterization of a therapeutic enzyme mutant with improved

DOI: 10.1021/acschemneuro.5b00001
ACS Chem. Neurosci. 2015, 6, 658−665

stability and function for cocaine detoxification. *ACS Chem. Biol. 9*, 1764−1772.
(52) Volkow, N. D., Wang, G. J., Fischman, M. W., Foltin, R. W., Fowler, J. S., Abumrad, N. N., Vitkun, S., Logan, J., Gatley, S. J., Pappas, N., Hitzemann, R., and Shea, C. E. (1997) Relationship between subjective effects of cocaine and dopamine transporter occupancy. *Nature 386*, 827−830.
(53) Kitayama, S., Shimada, S., Xu, H., Markham, L., Donovan, D. M., and Uhl, G. R. (1992) Dopamine transporter site-directed mutations differentially alter substrate transport and cocaine binding. *Proc. Natl. Acad. Sci. U.S.A. 89*, 7782−7785.
(54) Harrod, S., Mactutus, C., Fitting, S., Hasselrot, U., and Booze, R. (2008) Intra-accumbal Tat1−72 alters acute and sensitized responses to cocaine. *Pharmacol., Biochem. Behav. 90*, 723−729.
(55) Wang, G.-J., Chang, L., Volkow, N. D., Telang, F., Logan, J., Ernst, T., and Fowler, J. S. (2004) Decreased brain dopaminergic transporters in HIV-associated dementia patients. *Brain 127*, 2452−2458.
(56) Hsieh, P. C., Yeh, T. L., Lee, I. H., Huang, H. C., Chen, P. S., Yang, Y. K., Chiu, N. T., Lu, R. B., and Liao, M.-H. (2010) Correlation between errors on the Wisconsin Card Sorting Test and the availability of striatal dopamine transporters in healthy volunteers. *J. Psychiatry Neurosci. 35*, 90−94.
(57) Mozley, L. H., Gur, R. C., Mozley, P. D., and Gur, R. E. (2001) Striatal dopamine transporters and cognitive functioning in healthy men and women. *Am. J. Psychiatry 158*, 1492−1499.
(58) Robertson, K. R., Smurzynski, M., Parsons, T. D., Wu, K., Bosch, R. J., Wu, J., McArthur, J. C., Collier, A. C., Evans, S. R., and Ellis, R. J. (2007) The prevalence and incidence of neurocognitive impairment in the HAART era. *AIDS 21*, 1915−1921.
(59) Gelman, B. B., Lisinicchia, J. G., Chen, T., Johnson, K. M., Jennings, K., Freeman, D. H., Jr., and Soukup, V. M. (2012) Prefrontal dopaminergic and enkephalinergic synaptic accommodation in HIV-associated neurocognitive disorders and encephalitis. *J. Neuroimmune Pharmacol. 7*, 686−700.
(60) Giros, B., el Mestikawy, S., Godinot, N., Zheng, K., Han, H., Yang-Feng, T., and Caron, M. G. (1992) Cloning, pharmacological characterization, and chromosome assignment of the human dopamine transporter. *Mol. Pharmacol. 42*, 383−390.
(61) Beuming, T., Shi, L., Javitch, J. A., and Weinstein, H. (2006) A comprehensive structure-based alignment of prokaryotic and eukaryotic neurotransmitter/Na+ symporters (NSS) aids in the use of the LeuT structure to probe NSS structure and function. *Mol. Pharmacol. 70*, 1630−1642.
(62) Rudnick, G. (2011) Cytoplasmic Permeation Pathway of Neurotransmitter Transporters. *Biochemistry 50*, 7462−7475.
(63) Yamashita, A., Singh, S. K., Kawate, T., Jin, Y., and Gouaux, E. (2005) Crystal structure of a bacterial homologue of Na+/Cl−dependent neurotransmitter transporters. *Nature 437*, 215−223.
(64) Forrest, L. R., Tavoulari, S., Zhang, Y.-W., Rudnick, G., and Honig, B. (2007) Identification of a chloride ion binding site in Na +/Cl−dependent transporters. *Proc. Natl. Acad. Sci. U.S.A. 104*, 12761−12766.
(65) Zomot, E., Bendahan, A., Quick, M., Zhao, Y., Javitch, J. A., and Kanner, B. I. (2007) Mechanism of chloride interaction with neurotransmitter: sodium symporters. *Nature 449*, 726−730.
(66) Singh, S. K., Yamashita, A., and Gouaux, E. (2007) Antidepressant binding site in a bacterial homologue of neurotransmitter transporters. *Nature 448*, 952−956.
(67) Singh, S. K., Piscitelli, C. L., Yamashita, A., and Gouaux, E. (2008) A competitive inhibitor traps LeuT in an open-to-out conformation. *Science 322*, 1655−1661.
(68) Piscitelli, C. L., Krishnamurthy, H., and Gouaux, E. (2010) Neurotransmitter/sodium symporter orthologue LeuT has a single high-affinity substrate site. *Nature 468*, 1129−1132.
(69) Wang, H., Elferich, J., and Gouaux, E. (2012) Structures of LeuT in bicelles define conformation and substrate binding in a membrane-like context. *Nat. Struct. Mol. Biol. 19*, 212−219.
(70) Krishnamurthy, H., and Gouaux, E. (2012) X-ray structures of LeuT in substrate-free outward-open and apo inward-open states. *Nature 481*, 469−474.
(71) Penmatsa, A., Wang, K. H., and Gouaux, E. (2013) X-ray structure of dopamine transporter elucidates antidepressant mechanism. *Nature 503*, 85−90.
(72) Huang, X., and Zhan, C.-G. (2007) How dopamine transporter interacts with dopamine: insights from molecular modeling and simulation. *Biophys. J. 93*, 3627−3639.
(73) Kniazeff, J., Shi, L., Loland, C. J., Javitch, J. A., Weinstein, H., and Gether, U. (2008) An intracellular interaction network regulates conformational transitions in the dopamine transporter. *J. Biol. Chem. 283*, 17691−17701.
(74) Huang, X., Gu, H. H., and Zhan, C.-G. (2009) Mechanism for cocaine blocking the transport of dopamine: insights from molecular modeling and dynamics simulations. *J. Phys. Chem. B 113*, 15057−15066.
(75) Koldsø, H., Christiansen, A. B., Sinning, S., and Schiøtt, B. (2012) Comparative modeling of the human monoamine transporters: similarities in substrate binding. *ACS Chem. Neurosci. 4*, 295−309.
(76) Midde, N. M., Huang, X., Gomez, A. M., Booze, R. M., Zhan, C.-G., and Zhu, J. (2013) Mutation of tyrosine 470 of human dopamine transporter is critical for HIV-1 Tat-induced inhibition of dopamine transport and transporter conformational transitions. *J. Neuroimmune Pharmacol. 8*, 975−987.
(77) Šali, A., Potterton, L., Yuan, F., van Vlijmen, H., and Karplus, M. (1995) Evaluation of comparative protein modeling by MODELLER. *Proteins: Struct., Funct., Bioinf. 23*, 318−326.
(78) Nayeem, A., Sitkoff, D., and Krystek, S. (2006) A comparative study of available software for high-accuracy homology modeling: From sequence alignments to structural models. *Protein Sci. 15*, 808−824.
(79) Pierce, B. G., Hourai, Y., and Weng, Z. (2011) Accelerating protein docking in ZDOCK using an advanced 3D convolution library. *PLoS One 6*, e24657.
(80) Case, D. A., Darden, T. A., Cheatham Iii, T. E., Simmerling, C. L., Wang, J., Duke, R. E., Luo, R., Walker, R. C., Zhang, W., Merz, K. M., Roberts, B., Hayik, S., Roitberg, A., Seabra, G., Swails, J., Goetz, A. W., Kolossváry, I., Wong, K. F., Paesani, F., Vanicek, J., Wolf, R. M., Liu, J., Wu, X., Brozell, S. R., Steinbrecher, T., Gohlke, H., Cai, Q., Ye, X., Wang, J., Hsieh, M. J., Cui, G., Roe, D. R., Mathews, D. H., Seetin, M. G., Salomon-Ferrer, R., Sagui, C., Babin, V., Luchko, T., Gusarov, S., Kovalenko, A., and Kollman, P. A. (2012) *AMBER 12*, University of California, San Francisco.
(81) Péloponèse, J. M., Grégoire, C., Opi, S., Esquieu, D., Sturgis, J., Lebrun, E., Meurs, E., Collette, Y., Olive, D., Aubertin, A. M., Witvrow, M., Pannecouque, C., De Clercq, E., Bailly, C., Lebreton, J., and Loret, E. P. (2000) 1H-13C nuclear magnetic resonance assignment and structural characterization of HIV-1 Tat protein. *C. R. Acad. Sci. III 323*, 883−894.
(82) Miller, B. R., III, McGee, T. D., Jr., Swails, J. M., Homeyer, N., Gohlke, H., and Roitberg, A. E. (2012) MMPBSA. py: An efficient program for end-state free energy calculations. *J. Chem. Theory Comput. 8*, 3314−3321.
(83) Accelrys Software (2009) *Studio D, Version 2.5*, Accelrys, Inc., San Diego, CA.
(84) Dolinsky, T. J., Nielsen, J. E., McCammon, J. A., and Baker, N. A. (2004) PDB2PQR: an automated pipeline for the setup of Poisson−Boltzmann electrostatics calculations. *Nucleic Acids Res. 32*, W665−W667.
(85) Pierce, B., and Weng, Z. (2007) ZRANK: reranking protein docking predictions with an optimized energy function. *Proteins: Struct., Funct., Bioinf. 67*, 1078−1086.

DOI: 10.1021/acschemneuro.5b00001
ACS Chem. Neurosci. 2015, 6, 658−665